

Standing Enokitake-like Nanowire Films for Highly Stretchable Elastronics

Yan Wang,^{†,¶} Shu Gong,^{†,¶} Stephen J. Wang,^{¶,⊥} Xinyi Yang,[¶] Yunzhi Ling,[†] Lim Wei Yap,^{†,¶} Dashen Dong,[†] George P. Simon,[§] and Wenlong Cheng^{*,†,‡,⊥}

[†]Department of Chemical Engineering, [§]Department of Materials Science and Engineering, and [¶]International Tangible Interaction Design Lab, Monash University, Clayton, Victoria 3800, Australia

[‡]The Melbourne Centre for Nanofabrication, Clayton, Victoria 3800, Australia

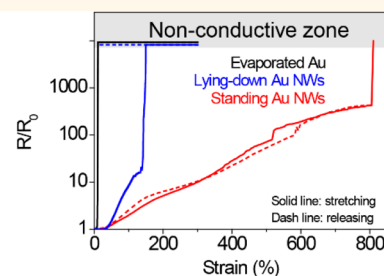
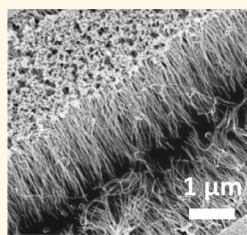
[⊥]Department of Innovation Design Engineering, School of Design, Royal College of Art, London SW7 2EU, United Kingdom

Supporting Information

ABSTRACT: Stretchable electronics may enable electronic components to be part of our organs—ideal for future wearable/implantable biodiagnostic systems. One of key challenges is failure of the soft/rigid material interface due to mismatching Young's moduli, which limits stretchability and durability of current systems. Here, we show that standing enokitake-like gold-nanowire-based films chemically bonded to an elastomer can be stretched up to 900% and are highly durable, with >93% conductivity recovery even after 2000 stretching/releasing cycles to 800% strain.

Both experimental and modeling reveal that this superior elastic property originates from standing enokitake-like nanowire film structures. The closely packed nanoparticle layer sticks to the top of the nanowires, which easily cracks under strain, whereas the bottom part of the nanowires is compliant with substrate deformation. This leads to tiny V-shaped cracks with a maintained electron transport pathway rather than large U-shaped cracks that are frequently observed for conventional metal films. We further show that our standing nanowire films can serve as current collectors in supercapacitors and second skin-like smart masks for facial expression detection.

KEYWORDS: standing nanowire film, unconventional crack, elastronics, electronic skins, strain sensors



Electronics are transitioning from the current rigid version to a next-generation flexible design, which will ultimately evolve into stretchable electronics (*i.e.*, elastronics). In an elastronic system, its components can be seamlessly integrated with skin/muscles to become parts of our organs, thereby enabling genuine biodiagnostics in real time and *in situ*. It is well-known that elastronics require a seamless combination of stretchability and electrical conductivity, which can be achieved extrinsically or intrinsically.^{1–3} The former is achieved by designing structures that stretch,^{4–10} whereas the latter is realized by producing materials that are deformable.^{11–22}

An ideal elastronic system may be made from intrinsically elastic components, including conductors, resistors, diodes, transistors, and sensors, so that they can integrate with modulus-matching skin/muscle,^{12–19,23,24} ideal for wearable/implantable diagnostics with true capability of health monitoring anytime and anywhere. A viable strategy is to deposit active nanomaterials onto or embed them into elastomers.^{12,14–17,25–33} Among them, one-dimensional nanomaterials are particularly promising as they can be used to construct percolation networks onto or into elastomeric

matrices.^{12,14,22,25–32,34} Two-dimensional (2D) percolation nanowire-based thin films have demonstrated a wide range of applications in wearable electronic skin (e-skin) sensors,³⁵ soft energy devices,^{36,37} organic light-emitting diodes,³⁸ memory devices,³⁹ PM 2.5 filters,⁴⁰ soft robotics,²⁶ and transparent electronics.^{41–46} Despite this encouraging progress, delamination and/or cracks at the soft/rigid materials' interface often occur under large or repeated strains due to mismatching Young's moduli between active rigid materials and soft elastomeric matrixes. This limits the stretchability and long-term durability of current systems, preventing them from being used in real-world applications.⁴⁷

In this work, we show that standing enokitake-like gold nanowire films chemically bonded to elastomeric materials can exhibit stretchability (up to 900%) much higher than that of conventional vacuum-evaporated bulk metal or percolating nanowire films, without any additional extrinsic buckling design. This was achieved because of standing enokitake-like

Received: July 3, 2018

Accepted: September 4, 2018

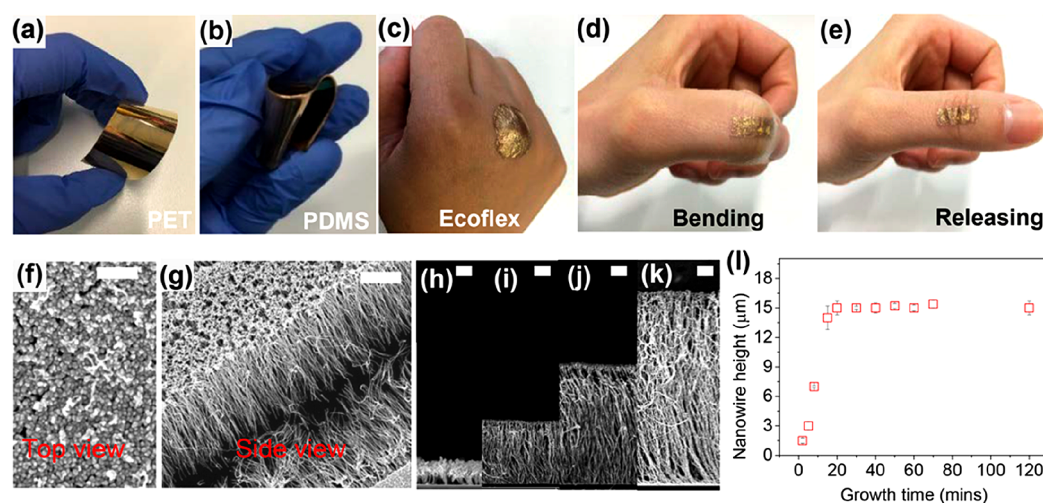


Figure 1. Characteristics of standing enokitake-like nanowire-based gold films. (a–c) Optical appearances of standing enokitake-like nanowire-based films grown on flat elastomers: (a) PET, (b) PDMS, (c) Ecoflex. (d,e) Photographs of the thin standing enokitake-like nanowire-based gold films on a human thumb knuckle while bending and releasing, respectively. (f,g) Typical top-view and side-view SEM image of standing enokitake-like nanowire-based gold films. Scale bar: 200 nm. (h–k) SEM images of standing nanowire films with different thicknesses: (h) $\sim 1.5 \mu\text{m}$, (i) $\sim 3.5 \mu\text{m}$, (j) $\sim 7 \mu\text{m}$, and (k) $\sim 14 \mu\text{m}$. Scale bar: $1 \mu\text{m}$. (l) Change of nanowire height as a function of growth time.

nanowire structures and their strong adhesion with elastomers, leading to distinct stretching behaviors. Unlike conventional metal films (by vacuum evaporation/sputtering or previous nanomaterials films) which typically exhibit large “cliff-like” “U-shaped” cracks that cannot recover upon releasing the strain, our standing enokitake-like nanowire gold films instead show tiny “V-shaped” cracks that are able to recover the conductivity when strain is removed. The formation of V-shaped cracks is due to hierarchical structures of the nanowire film, in which the top nanoparticle layer is mechanically more rigid than the underlying nanowire layer. This leads to initial cracking that starts from the top particle layer under low level of strains (typically below 300%), followed by conventional large U-shaped cracks of the entire film under large strains (typically between 300 and 800%). In both cases, conductivity pathways could be maintained. This unconventional property enables our enokitake-like nanowire film to be used as highly durable conductors which could retain the $>93\%$ conductance even after 2000 stretching/releasing cycles to 800% strain. We demonstrate specifically here that they can be applied to fabricate intrinsically stretchable supercapacitors and can be used as “second-skin” facial expression recognition mask sensors.

RESULTS AND DISCUSSION

By extending the method of seed-mediated electroless plating on rigid surfaces,⁴⁸ standing enokitake-like nanowire-based gold films could grow on a number of polymer substrates including polyethylene terephthalate (PET), polydimethylsiloxane (PDMS), and Ecoflex (highly stretchy silicone rubber). Macroscopically, the standing nanowire films were uniform with a shiny gold reflective surface if the underlying elastomeric substrates were flat (Figure 1a–c). The fabrication process is illustrated in Figure S1. In brief, an elastomeric substrate is first treated using O_2 plasma to render its surface hydrophilic, which is then followed by silanization with (3-aminopropyl)trimethoxysilane (APTMS). Next, negatively charged seed particles could be immobilized onto this amine-functionalized surfaces *via* electrostatic attraction. Further

immersion of the seed-particle-modified elastomer into a growth solution containing gold precursors, surfactants, and reducing agents could lead to the formation of densely packed standing nanowire arrays. The gold films grown on thin Ecoflex sheets ($\sim 20 \mu\text{m}$ thickness) could naturally attach to human skin wrinkles before and after stretching (Movie S1). The growth process was found to be scalable and able to conformably coat a range of other polymer substrates from macroscopic to microscopic (Figure S2a–f) and even to textured skin replicas (Figure 1d,e and Figure S2g). Superior skin conformal attachment in conjunction with chemical inertness and biocompatibility of gold indicates the great potential of our nanowire film as second skin patches for various biomedical applications.

Further top-view and side-view characterizations by scanning electron microscopy (SEM) revealed enokitake-like nanowire film structures (Figure 1f,g), in which the top layer (“head” side) consists of closely packed gold nanoparticles with a diameter of $9.3 \pm 2.1 \text{ nm}$. The bottom layer (“tail” side) is composed of nanowires standing normal to the elastomer substrates, with a typical nanowire diameter of $7.8 \pm 1.7 \text{ nm}$. In addition, the number density of nanowires can reach as high as $\sim 1.09 \times 10^4 \mu\text{m}^{-2}$, which is much higher than that of previously reported 2D nanowire percolation network systems.^{35–39} The estimated porosity of the head side is 65–72%, whereas the tail side is 50–55%. Longer growth times lead to longer nanowires but reach the plateau in about 20 min (SEM images in Figure 1h–k). We obtained nanowires that were much longer than those in the literature⁴⁸ by using concentrated growth solution to achieve tunable lengths up to $\sim 15 \mu\text{m}$ (Figure 1l). In addition, the diameter of both nanoparticle and nanowire did not change much as the nanowire became longer (Figure S3). It is even possible to grow staircase-like nanowire films by mask-assisted step growth (Figure S4). Overall, the structural features including accurate height control, standing enokitake-like configuration, and control over surface topological structures indicate that our system is different from a dominant nanowire percolation

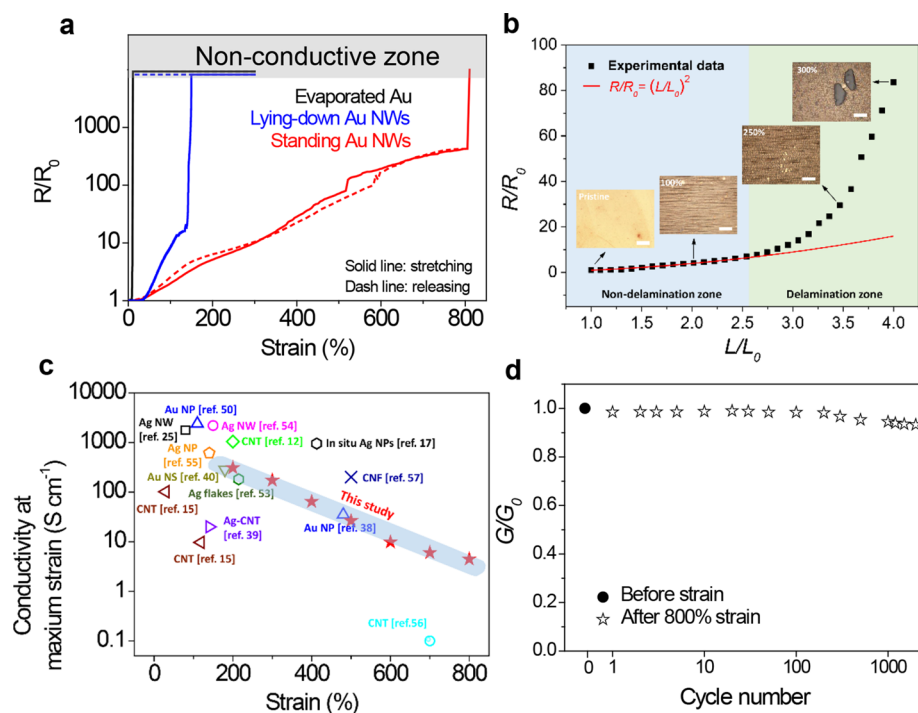


Figure 2. Superior intrinsic stretchability of standing enokitake-like nanowire-based gold films. (a) Comparison of stretchability among evaporated Au films, lying-down gold nanowire film and standing enokitake-like nanowire-based gold film. (b) Plot of normalized resistance (R/R_0) versus normalized length (L/L_0). Scattered black squares denote experimental data; the red curve is the theoretical prediction based on the equation $R/R_0 = (L/L_0)^2$. Inset: Representative optical images of standing nanowire film under different strains of 0, 100, 250, and 300%. Scale bar: $20\ \mu\text{m}$. (c) Comparison of this work to recent work in elastic conductors. Data points are extracted from the following papers: blue open triangle, Au nanoparticles (Au NPs);⁵⁰ pink open circle, Ag nanowires (Ag NWs);⁵⁴ black open square, Ag nanowires;²⁵ lime open diamond, carbon nanotube (CNT);¹² black open pentagon, *in situ* Ag NPs;¹⁷ orange open pentagon, Ag nanoparticles (Ag NPs);⁵⁵ pistachio open inverted triangle, Au nanosheets (Au NSs);⁴⁰ Royal cross, carbon nanofibers (CNFs);⁵⁷ green open pentagon, Ag flakes;⁴¹ sienna left open triangle, CNT;¹⁵ purple open right triangle, Ag carbon nanotubes (Ag CNT);⁴⁰ cyan open circle, CNT;⁵⁶ red filled star, this study. (d) Conductance change of standing enokitake-like nanowire-based film during 2000 stretching/releasing cycles up to 800% strain.

network^{26,35–39,46} and may be viewed as a three-dimensional percolation system.

We systematically investigate stretchability of the standing nanowire-based film. When directly grown on Ecoflex substrates with the nanowire chemically bound to surfaces, the films exhibit exceptionally high stretchability up to 800% of strain (Figure 2a, red solid line). With additional Ecoflex encapsulation, the conductivity was observed to survive even at the 900% strain, which is almost the physical limit of the Ecoflex elastomer (Figure S5). The improved stretchability with Ecoflex encapsulation may be due to the enhanced bonding at the top side, leading to more uniform crack propagation of the nanoparticle, preventing catastrophic failure. This observation is in agreement with sandwiched silver-nanowire-percolated structure reported previously.⁴⁹ Remarkably, the original conductivity could be recovered upon stress release (Figure 2a, red dashed line). In control experiments, we found that the evaporated gold can only survive $\sim 10\%$ strain before conductivity is lost, and the percolation lying-down nanowire film is only able to tolerate a $\sim 150\%$ strain (blue solid line in Figure 2a). Both bulk metal and percolation nanowire films show no conductivity recovery upon stress release (black and blue dashed lines in Figure 2a). We further plot normalized resistance (R/R_0) versus normalized length square (L/L_0)² for experimental data collection and theoretical prediction (Figure 2b), where R_0 and L_0 are the resistance and length, respectively, of samples at 0% strain. The deviation starts at a strain of $\sim 150\%$, above

which cracks form and propagate, which is further validated from optical imaging (inset of Figure 2b). This threshold value is 3-fold that for copper-bonded Kapton film.⁴⁷ Note that 800% stretchability for an enokitake-like standing nanowire film outperforms the state-of-the-art inorganic stretchable conducting film^{12,15,17,25,50–57} (Figure 2c). Remarkably, the film conductance G retained $>93\%$ of the initial conductance (G_0) after stretching/releasing to 800% strain for 2000 cycles (Figure 2d). This has not yet been achieved, to the best of our knowledge, by previously reported stretchable conductors without using prestrain or buckling designs.

We further established that strong adhesion between the nanowire and Ecoflex substrate and “accordion-fan-like” V-shaped cracking processes is responsible for the exceptional high stretchability observed. The adhesion test (Movie S2) clearly shows that our standing enokitake-like nanowire film could survive in the normal Scotch tape test multiple times without significant resistance change. The strong adhesion may be due to the use of APTMS that serves a bifunctional molecular glue. Its amine side strongly interacts with gold nanowires, and its silane sides covalently bond to Ecoflex surfaces. The introduction of an organic intermediate layer has been demonstrated as an effective strategy to improve the adhesion between the metallic layer and polymeric substrates, thus enhancing the overall performance of the stretchable conductive film.^{58–61} Unlike the continuous bulk metal film, our nanophased enokitake-like structures offer better stretchability (Table S1).

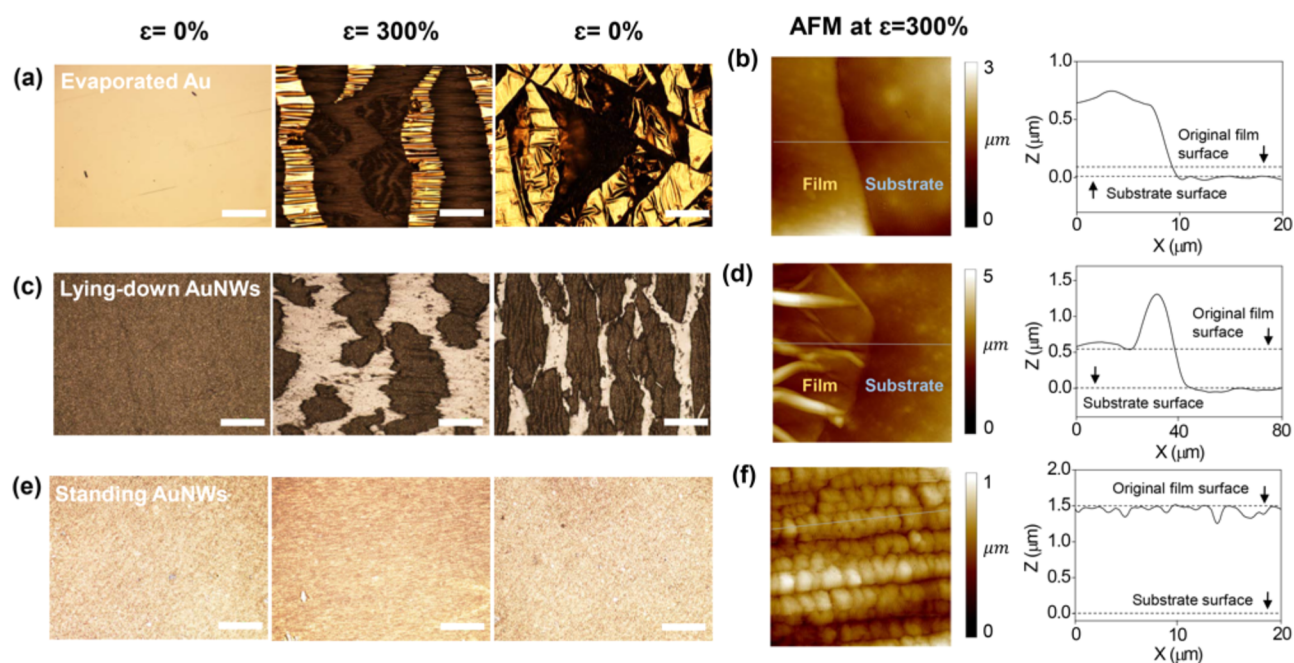


Figure 3. Optical microscopic and AFM characteristics of three different gold films (evaporated gold film, lying-down nanowire gold film, and standing enokitake-like nanowire-based gold film). Microscopic behavior of (a) evaporated Au film, (c) lying-down nanowire gold film, and (e) standing enokitake-like nanowire-based gold film by optical microscope imaging at various strain (from 0, 300, and back to 0%), respectively. AFM images and height plots of (b) evaporated gold film, (d) lying-down nanowire gold film, and (f) standing enokitake-like nanowire-based gold film under 300% strain. Nanowire height for standing enokitake-like nanowire-based gold film is 1.5 μm . Scale bar: 200 μm . All optical images have the same resolution.

Unlike conventional bulk gold or percolation nanowire films, our standing nanowire films have hierarchical structures with close-packed nanoparticle arrays on the top and aligned nanowires chemically bound to elastomeric substrates. This leads to a distinct stretching mechanism (Figure S6). For further investigation, we carried out detailed multiscale morphological studies in order to understand the exceptional stretchability observed. We scrutinized morphological features in different locations of rectangle standing nanowire metallic nanopatches under various strains by optical microscopy (Figure S7). This offers a panoramic overview of our standing nanowire film stretching process at millimeter and micrometer length scales. Evident cracks will not be seen until about 300% strain is applied. At the nanoscale, atomic force microscopy (AFM) and cross-sectional SEM characterization under a stretched state clearly show the presence of V-shaped cracks (Figures S8 and S9). The cracking depths measured for the two particular standing nanowire films under different strains were significantly lower than the film thickness. Assuming that the nanowire deforms elastically without breaking up and with its ends firmly attached to elastomeric substrates, we can visualize a V-shaped cracking process by finite element analysis (Movie S3). However, both bulk gold films and percolation nanowire films exhibit only typical U-shaped cracks (Figure 3a–d; also see Figure S10 for the schematic illustration of V-shaped crack and U-shaped crack). Both can tolerate a level of strain much less than that for the standing nanowire films. The concurrent film delamination prevents recovery of original structures, hence, leading to poor conductivity recovery (Figure S6a,b). Note that the stretching mechanism of our nanowire film is fundamentally different from previous aligned carbon nanotube arrays where building blocks were not

standing normal to the substrate but were lying down flush on the substrate.³⁰

The above multiscale structural characterizations and finite elemental analysis reveal the following mechanistic insights. Cracks initiate from the head side, which serve as unzipping points for strongly bundling nanowire arrays, yet the interacting nanowire tail ends deform conformably to the substrate without cracking (Figure 3e,f and Figure S6c). At the point when substrate elongation commences, the mechanically rigid top gold nanoparticle layer (head side) cracks, which triggers the formation of V-shaped cracks as the strain level is increased by unzipping them from the top side. This typically occurs when the strain level is less than $\sim 150\%$ strain, where no delamination occurs between substrates and our gold film at this stage. Obvious wrinkles are observed in the middle part of the standing nanowire film because of the Poisson ratio of Ecoflex substrate (Figure S7, middle left). As the strain increases further to a certain threshold, large U-shaped cracks form as a result of the standing nanowire film sliding/delaminating from the supporting elastomeric substrates. The U-shaped cracks propagate as the strain level is further increased; however, percolation conductive pathways are still maintained until reaching a catastrophic failing point. The V-shaped and U-shaped cracks coexist at the high strain levels typically from 300 to 800%. The self-repairable cracks were also demonstrated from more detailed SEM characterization. By inspecting the same spot in a particular sample, negligible morphological changes were observed before and after 60 000 cycles of stretching/releasing to 185% strain (Figure S11). Its excellent stretchability was maintained even after 40 weeks of storage in ambient conditions without encapsulation (Figure S12).

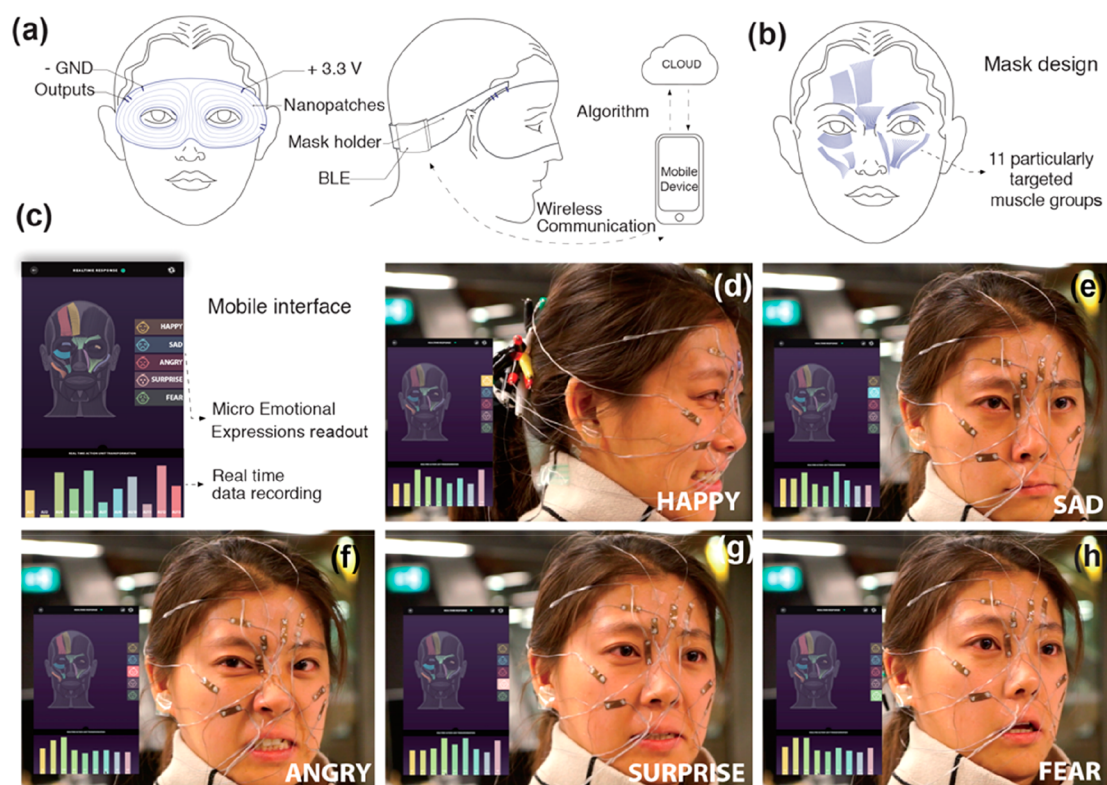


Figure 4. Real-time facial expressions monitoring. (a) Schematic illustration of the detection system setup. (b) Schematic of standing enokitake-like nanowire-based gold film smart mask design according to nine facial muscle group movements caused by various emotions. (c) Mobile device interface for result reading. (d–h) Real-time monitoring of five different facial expressions of happy, sad, angry, surprise, and fear.

We also found that the stretchability of the standing nanowire film showed a decreasing trend, whereas nanowire length increased (Figure S13a). As the nanowire length increased to 14 μm , the film lost conductivity at 80% strain, which is 10 times lower than that of the 1.5 μm film. As expected, the overall nanowire/Ecoflex sheet became stiffer as the nanowire length increased (Figure S13b). This could be due to strong wire-to-wire interactions among longer nanowires, rendering nanowire films more rigid, approaching bulk gold mechanical properties.

The facile growth of a standing nanowire film in conjunction with their outstanding performances indicates their suitability for soft electronics applications. As the first proof of concept, we demonstrate their use in soft, stretchable supercapacitors using our gold film with short nanowires. In a typical symmetrical layout, we were able to achieve excellent capacitive behavior (Figure S14), which also shows negligible changes over a wide range of applied tensile strain from 0 to 250%. The slight capacitance increase from 0 to 100% strain may be due to increased surface area of the nanowire unzipping process under strain. Further stretching beyond the 100% strain caused a very small decrease in the capacitance, retaining 84% of the original capacitance at a strain up to 250% (Figure S15a,b). This slight degradation of capacitance is possibly due to the conductivity decreases of standing nanowire film electrodes and/or deformation of the electrolyte layers over stretching. Nevertheless, specific capacitance could be maintained by 99% after 200 stretch/release cycles at the strain of 200%, suitable for wearable on-body energy storage devices (Figure S15c,d).

The excellent skin conformability of our standing nanowire film enabled its use as e-skin smart nanopatches for detecting childhood autism disorder. Note that the smart nanopatches were fabricated by a strain-sensitive film from longer standing nanowires. Instead of an optical approach used by the NODA diagnostic tool available on Apple store, we used nine e-skin nanopatches to monitor particular pieces of muscle/skin stretching related to facial expression (Figure 4). Based on the information from the Facial Action Coding System (FACS) library from Ekman's group,⁶² we could relate electrical signals to the five different emotional expressions (happy, sad, angry, surprise, and fear) in a wireless manner (Movie S4). Different facial expressions can be read from a mobile screen in real time.

CONCLUSIONS

In summary, we report the exceptional high stretchability and durability of standing enokitake-like nanowire-based gold films, which are unexpected in the context of current dominant nanowire percolation network-based stretchable conductors. Our results clearly reveal that this is attributed to standing enokitake-like nanowire structures, vertically aligned configuration, and strong chemical bonding interactions between standing nanowire films and elastomeric substrates. Together, this leads to distinct elastic properties that have never been observed for conventional bulk metal films or other nanomaterial networks (both vertically aligned and lying-down aligned carbon-nanotube-based systems; see Table S2 in the Supporting Information). We further demonstrate the applications of our standing nanowire film in stretchable supercapacitors and wearable e-skin sensors, beyond which we

may find a myriad of additional applications in future elastronics.

METHODS

Chemicals. Gold(III) chloride trihydrate ($\text{HAuCl}_4 \cdot 3\text{H}_2\text{O}$, 99.9%), triisopropylsilane (99%), 4-mercaptobenzoic acid (MBA, 90%), APTMS, sodium citrate tribasic dihydrate (99.0%), L-ascorbic acid, poly(vinyl alcohol) (PVA) powder, H_3PO_4 , and ethanol (analytical grade) were purchased from Sigma-Aldrich. All solutions were prepared using deionized water (resistivity $>18 \text{ M}\Omega \cdot \text{cm}^{-1}$). All chemicals were used as received unless otherwise indicated. Conductive wires were purchased from Adafruit.

Elastomeric Substrates. PDMS substrates were made by mixing Sylgard 184 silicone elastomer base and curing agent at a weight ratio of 10:1. The mixture was poured on a 6 in. flat-plate Petri dish using 0.5 mm height shims as spacers and cured at 65°C for 2 h in an oven. Ecoflex substrates were made by pouring Ecoflex curable silicone fluid (Smooth-On Ecoflex 00-30) into a 6 in. flat-plate Petri dish and curing under room temperature for 4 h.

Synthesis of Standing Gold Nanowire Films. A modified seed-mediated approach was used, as described in the literature.⁸ First, 2 nm seed gold nanoparticles were synthesized. Briefly, 0.147 mL of 34 mM sodium citrate was added into a conical flask with 20 mL of H_2O under vigorous stirring. After 1 min, 600 μL of ice-cold, freshly prepared 0.1 M NaBH_4 solution was added with stirring. The solution turned brown immediately. The solution was then stirred for 5 min and stored at 4°C until needed.

To grow standing nanowires on substrates (e.g., Si wafer, Ecoflex), O_2 plasma was applied to render the surfaces hydrophilic. Depending on the types of substrates, the plasma treatment time varied from 2 to 17 min. Then the substrates were functionalized with an amino group by silanization reaction with 5 mM APTMS solution for 1 h. APTMS-modified substrates were immersed into excess citrate-stabilized Au seed (3–5 nm) solution for 2 h to ensure the saturated adsorption of gold seeds, followed by rinsing with water four times to remove the weakly bound seed particles. Finally, seed-particle-anchored substrates were in contact with a growth solution containing 980 μM MBA, 12 mM HAuCl_4 , and 29 mM L-ascorbic acid, leading to the formation of standing nanowire films. The length of nanowires depended on the growth reaction time. Typical nanowire heights of ~ 1.5 , ~ 3.5 , ~ 5 , ~ 7 , and $\sim 14 \mu\text{m}$ were obtained by adjusting the growth time to 2, 4, 5, 8, and 15 min, respectively.

Lying-Down Gold Nanowire Films. $\text{HAuCl}_4 \cdot 3\text{H}_2\text{O}$ (44 mg) was added into 40 mL of hexane, followed by addition of 1.5 mL of oleylamine. After the gold salts were completely dissolved, 2.1 mL of triisopropylsilane was added into the above solution. The resulting solution was left to stand for 2 days without stirring at room temperature until the color turned from yellow to dark brown, indicating the formation of gold nanowires. The chemical residues were removed by repeated centrifugation and thorough washing using ethanol/hexane (3/1, v/v) and finally concentrated to a 2 mL stock solution in hexane. The lying-down gold nanowire films could then be obtained by a simple drop-casting approach.

Vacuum-Evaporated Gold Film. A 100 nm gold film could be obtained using an e-beam evaporator (Intlvac Nanochrome II, 10 kV).

Characterization. SEM imaging was carried out using a FEI Helios Nanolab 600 FIB-SEM operating at a voltage of 5 kV. The sheet resistances of the standing enokitake-like nanowire-based gold films were carried out on a Jandel four-point conductivity probe by using a linear arrayed four-point head. To test the electromechanical responses for strain and bending sensing, the two ends of the samples were attached to motorized moving stages (THORLABS model LTS150/M). Uniform stretching/bending cycles were applied by a computer-based user interface (Thorlabs APT user), and the current changes were measured by the Parstat 2273 electrochemical system (Princeton Applied Research). For the analysis of detailed point load or pressure responses, a computer-based user interface and a force sensor (ATI Nano17 force/torque sensor) and a Maxon Brushless

DC motor using a high-resolution quadrature encoder ($15 \mu\text{m}$ of linear resolution) were used to apply an external point load or pressure. Ecoflex with a thickness of $500 \mu\text{m}$ was chosen as the substrate of the standing nanowire film in a strain test. PET with a thickness of $125 \mu\text{m}$ was chosen as the substrate of the standing nanowire film in a strain test. PDMS with a thickness of 1 mm was chosen as the substrate of the standing nanowire film in a point load/pressure test. The reflectance (R) data were collected from a PerkinElmer UV-vis-NIR spectrophotometer (Lambda 1050) with an integrating sphere setup.

Simulation. The finite element analysis model was implemented in the ABAQUS 6.14/Standard software. Ecoflex substrate was meshed using structured hex elements, whereas gold nanowires were used a tetrahedral elements. There were a total of 2640 linear hexahedral elements in the Ecoflex substrate and 106 200 quadratic tetrahedral elements in the gold nanowire section. The aspect ratio of the gold nanowire was modeled at 100, with a length of 800 nm and a diameter of 8 nm. The elastic modulus and Poisson's ratio are 400 kPa and 0.49 for the Ecoflex substrate and 70 GPa and 0.42 for nanowire, respectively. The boundary conditions were set by fixing the left end of Ecoflex substrate and stretching uniaxially to 800% elongation. The contact condition between the nanowire layer and Ecoflex substrate was assumed to be pinned using a tie constraint.

Elastic Supercapacitors. The standing enokitake-like nanowire-based gold film was cut into small pieces with suitable shapes and sizes. A gel solution that contained PVA powder (1.0 g) and H_3PO_4 (1.0 g) in water (10.0 mL) was coated on top of the prepared films and dried in air for 5 h. Then two such-prepared standing enokitake-like nanowire-based gold film electrodes were assembled with sandwiched electrolytes to form a symmetrical electrochemical capacitor.

Wireless Facial Expression Monitoring. The circuit was composed of nine standing enokitake-like nanowire-based gold film sensors for measuring 11 facial muscle groups, and the supporting circuit was constructed with 3.3 V power supply and 13 330 Ω resistors. After the standing enokitake-like nanowire-based gold film sensors were mounted on the particularly targeted muscle groups on the subject's face, electrical responses of each sensor were recorded. A Bluetooth low energy technology was used to transfer the analogue reading data of each sensor to an Android OS-equipped mobile device (e.g., phone or pad style device). A specially designed app, already installed on the mobile device, first went through a machine learning session, which was referenced to the FACS library from Ekman's group. The FACS contributes as the reference blueprint for pattern recognitions to detect various facial expressions. This system was able to process electrical responses from facial muscle groups in real time, provided the baseline for measuring subject's detailed facial movement, and eventually translated it to different emotional expressions. The system was also able to create a data dictionary to store the data based on the nine sensor readings to specific muscle groups.

ASSOCIATED CONTENT

Supporting Information

The Supporting Information is available free of charge on the ACS Publications website at DOI: 10.1021/acsnano.8b05019.

Movie S1: Thin standing enokitake-like nanowire films on the back of a human hand, stretching and releasing (AVI)

Movie S2: Repeatable adhesion tape test (AVI)

Movie S3: Finite element analysis modeling of strain deformation for standing nanowire film (AVI)

Movie S4: Wireless facial expression monitoring from standing nanowire-based smart sensors (AVI)

Figures S1–S15, Notes S1 and S2, Tables S1 and S2, and additional references (PDF)

AUTHOR INFORMATION

Corresponding Author

*E-mail: wenlong.cheng@monash.edu.

ORCID 

Lim Wei Yap: 0000-0003-3072-6307

Wenlong Cheng: 0000-0002-2346-4970

Author Contributions

[†]Y.W. and S.G. contributed equally to this work.

Notes

The authors declare no competing financial interest.

ACKNOWLEDGMENTS

This work was performed in part at the Melbourne Centre for Nanofabrication (MCN) in the Victorian Node of the Australian National Fabrication Facility (ANFF). This work is financially supported by ARC Discovery Projects DP180101715 and LP160100521.

REFERENCES

- (1) Rogers, J. A.; Someya, T.; Huang, Y. Materials and Mechanics for Stretchable Electronics. *Science* **2010**, *327*, 1603–1607.
- (2) Gong, S.; Cheng, W. Toward Soft Skin-Like Wearable and Implantable Energy Devices. *Adv. Energy Mater.* **2017**, *7*, 1700648.
- (3) Kim, D. H.; Xiao, J.; Song, J.; Huang, Y.; Rogers, J. A. Stretchable, Curvilinear Electronics Based on Inorganic Materials. *Adv. Mater.* **2010**, *22*, 2108–2124.
- (4) Khang, D.-Y.; Jiang, H.; Huang, Y.; Rogers, J. A. A Stretchable Form of Single-Crystal Silicon for High-Performance Electronics on Rubber Substrates. *Science* **2006**, *311*, 208–212.
- (5) Kaltenbrunner, M.; Sekitani, T.; Reeder, J.; Yokota, T.; Kuribara, K.; Tokuhara, T.; Drack, M.; Schwödiauer, R.; Graz, I.; Bauer-Gogonea, S.; et al. An Ultra-Lightweight Design for Imperceptible Plastic Electronics. *Nature* **2013**, *499*, 458–463.
- (6) Liu, Z.; Fang, S.; Moura, F.; Ding, J.; Jiang, N.; Di, J.; Zhang, M.; Lepró, X.; Galvão, D.; Haines, C.; et al. Hierarchically Buckled Sheath-Core Fibers for Superelastic Electronics, Sensors, and Muscles. *Science* **2015**, *349*, 400–404.
- (7) Xu, S.; Zhang, Y.; Cho, J.; Lee, J.; Huang, X.; Jia, L.; Fan, J. A.; Su, Y.; Su, J.; Zhang, H.; et al. Stretchable Batteries with Self-Similar Serpentine Interconnects and Integrated Wireless Recharging Systems. *Nat. Commun.* **2013**, *4*, 1543.
- (8) Song, Z.; Ma, T.; Tang, R.; Cheng, Q.; Wang, X.; Krishnaraju, D.; Panat, R.; Chan, C. K.; Yu, H.; Jiang, H. Origami Lithium-Ion Batteries. *Nat. Commun.* **2014**, *5*, 3140.
- (9) White, M. S.; Kaltenbrunner, M.; Glowacki, E. D.; Gutnichenko, K.; Kettlgruber, G.; Graz, I.; Aazou, S.; Ulbricht, C.; Egbe, D. A. M.; Miron, M. C.; Major, Z.; Scharber, M. C.; Sekitani, T.; Someya, T.; Bauer, S.; Sariciftci, N. S. Ultrathin, Highly Flexible and Stretchable PLEDs. *Nat. Photonics* **2013**, *7*, 811–816.
- (10) Niu, Z.; Dong, H.; Zhu, B.; Li, J.; Hng, H. H.; Zhou, W.; Chen, X.; Xie, S. Highly Stretchable, Integrated Supercapacitors Based on Single-Walled Carbon Nanotube Films with Continuous Reticulate Architecture. *Adv. Mater.* **2013**, *25*, 1058–1064.
- (11) Kim, K. S.; Zhao, Y.; Jang, H.; Lee, S. Y.; Kim, J. M.; Kim, K. S.; Ahn, J.-H.; Kim, P.; Choi, J.-Y.; Hong, B. H. Large-Scale Pattern Growth of Graphene Films for Stretchable Transparent Electrodes. *Nature* **2009**, *457*, 706–710.
- (12) Lipomi, D. J.; Vosgueritchian, M.; Tee, B. C.; Hellstrom, S. L.; Lee, J. A.; Fox, C. H.; Bao, Z. Skin-Like Pressure and Strain Sensors Based on Transparent Elastic Films of Carbon Nanotubes. *Nat. Nanotechnol.* **2011**, *6*, 788–792.
- (13) Wang, Y.; Zhu, C.; Pfattner, R.; Yan, H.; Jin, L.; Chen, S.; Molina-Lopez, F.; Lissel, F.; Liu, J.; Rabiah, N. I.; et al. A Highly Stretchable, Transparent, and Conductive Polymer. *Sci. Adv.* **2017**, *3*, e1602076.
- (14) Liang, J.; Li, L.; Niu, X.; Yu, Z.; Pei, Q. Elastomeric Polymer Light-Emitting Devices and Displays. *Nat. Photonics* **2013**, *7*, 817–824.
- (15) Sekitani, T.; Nakajima, H.; Maeda, H.; Fukushima, T.; Aida, T.; Hata, K.; Someya, T. Stretchable Active-Matrix Organic Light-Emitting Diode Display Using Printable Elastic Conductors. *Nat. Mater.* **2009**, *8*, 494–499.
- (16) Miyamoto, A.; Lee, S.; Cooray, N. F.; Lee, S.; Mori, M.; Matsuhisa, N.; Jin, H.; Yoda, L.; Yokota, T.; Itoh, A.; Sekino, M.; Kawasaki, H.; Ebihara, T.; Amagai, M.; Someya, T. Inflammation-Free, Gas-Permeable, Lightweight, Stretchable on-Skin Electronics with Nanomeshes. *Nat. Nanotechnol.* **2017**, *12*, 907–913.
- (17) Matsuhisa, N.; Inoue, D.; Zalar, P.; Jin, H.; Matsuba, Y.; Itoh, A.; Yokota, T.; Hashizume, D.; Someya, T. Printable Elastic Conductors by *in Situ* Formation of Silver Nanoparticles from Silver Flakes. *Nat. Mater.* **2017**, *16*, 834–840.
- (18) Keplinger, C.; Sun, J.-Y.; Foo, C. C.; Rothmund, P.; Whitesides, G. M.; Suo, Z. Stretchable, Transparent, Ionic Conductors. *Science* **2013**, *341*, 984–987.
- (19) Muth, J. T.; Vogt, D. M.; Truby, R. L.; Mengüç, Y.; Kolesky, D. B.; Wood, R. J.; Lewis, J. A. Embedded 3d Printing of Strain Sensors within Highly Stretchable Elastomers. *Adv. Mater.* **2014**, *26*, 6307–6312.
- (20) Tavakoli, M.; Malakooti, M. H.; Paisana, H.; Ohm, Y.; Green Marques, D.; Alhais Lopes, P.; Piedade, A. P.; de Almeida, A. T.; Majidi, C. Egan-Assisted Room-Temperature Sintering of Silver Nanoparticles for Stretchable, Inkjet-Printed, Thin-Film Electronics. *Adv. Mater.* **2018**, *30*, 1801852.
- (21) Wang, J.; Cai, G.; Li, S.; Gao, D.; Xiong, J.; Lee, P. S. Printable Superelastic Conductors with Extreme Stretchability and Robust Cycling Endurance Enabled by Liquid-Metal Particles. *Adv. Mater.* **2018**, *30*, 1706157.
- (22) Jin, J.; Lee, D.; Im, H. G.; Han, Y. C.; Jeong, E. G.; Rolandi, M.; Choi, K. C.; Bae, B. S. Chitin Nanofiber Transparent Paper for Flexible Green Electronics. *Adv. Mater.* **2016**, *28*, 5169–5175.
- (23) Chen, G.; Matsuhisa, N.; Liu, Z.; Qi, D.; Cai, P.; Jiang, Y.; Wan, C.; Cui, Y.; Leow, W. R.; Liu, Z.; et al. Plasticizing Silk Protein for on-Skin Stretchable Electrodes. *Adv. Mater.* **2018**, *30*, 1800129.
- (24) Wang, Y.; Gong, S.; Wang, S. J.; Simon, G. P.; Cheng, W. Volume-Invariant Ionic Liquid Microbands as Highly Durable Wearable Biomedical Sensors. *Mater. Horiz.* **2016**, *3*, 208–213.
- (25) Xu, F.; Zhu, Y. Highly Conductive and Stretchable Silver Nanowire Conductors. *Adv. Mater.* **2012**, *24*, 5117–5122.
- (26) Gong, S.; Lai, D. T. H.; Su, B.; Si, K. J.; Ma, Z.; Yap, L. W.; Guo, P.; Cheng, W. Highly Stretchy Black Gold E-Skin Nanopatches as Highly Sensitive Wearable Biomedical Sensors. *Adv. Electron. Mater.* **2015**, *1*, 1400063.
- (27) Lee, P.; Lee, J.; Lee, H.; Yeo, J.; Hong, S.; Nam, K. H.; Lee, D.; Lee, S. S.; Ko, S. H. Highly Stretchable and Highly Conductive Metal Electrode by Very Long Metal Nanowire Percolation Network. *Adv. Mater.* **2012**, *24*, 3326–3332.
- (28) Song, J.; Li, J.; Xu, J.; Zeng, H. Superstable Transparent Conductive Cu@Cu₄Ni Nanowire Elastomer Composites against Oxidation, Bending, Stretching, and Twisting for Flexible and Stretchable Optoelectronics. *Nano Lett.* **2014**, *14*, 6298–6305.
- (29) Lee, P.; Ham, J.; Lee, J.; Hong, S.; Han, S.; Suh, Y. D.; Lee, S. E.; Yeo, J.; Lee, S. S.; Lee, D.; Ko, S. H. Highly Stretchable or Transparent Conductor Fabrication by a Hierarchical Multiscale Hybrid Nanocomposite. *Adv. Funct. Mater.* **2014**, *24*, 5671–5678.
- (30) Yamada, T.; Hayamizu, Y.; Yamamoto, Y.; Yomogida, Y.; Izadi-Najafabadi, A.; Futaba, D. N.; Hata, K. A Stretchable Carbon Nanotube Strain Sensor for Human-Motion Detection. *Nat. Nanotechnol.* **2011**, *6*, 296–301.
- (31) Lee, P.; Lee, J.; Lee, H.; Yeo, J.; Hong, S.; Nam, K. H.; Lee, D.; Lee, S. S.; Ko, S. H. Highly Stretchable and Highly Conductive Metal Electrode by Very Long Metal Nanowire Percolation Network. *Adv. Mater.* **2012**, *24*, 3326–3332.
- (32) Han, S.; Hong, S.; Ham, J.; Yeo, J.; Lee, J.; Kang, B.; Lee, P.; Kwon, J.; Lee, S. S.; Yang, M. Y.; et al. Fast Plasmonic Laser

Nanowelding for a Cu-Nanowire Percolation Network for Flexible Transparent Conductors and Stretchable Electronics. *Adv. Mater.* **2014**, *26*, 5808–5814.

(33) Yamada, T.; Hayamizu, Y.; Yamamoto, Y.; Yomogida, Y.; Izadi-Najafabadi, A.; Futaba, D. N.; Hata, K. A Stretchable Carbon Nanotube Strain Sensor for Human-Motion Detection. *Nat. Nanotechnol.* **2011**, *6*, 296–301.

(34) Sun, H.; You, X.; Deng, J.; Chen, X.; Yang, Z.; Chen, P.; Fang, X.; Peng, H. A Twisted Wire-Shaped Dual-Function Energy Device for Photoelectric Conversion and Electrochemical Storage. *Angew. Chem., Int. Ed.* **2014**, *53*, 6664–6668.

(35) Kim, K. K.; Hong, S.; Cho, H. M.; Lee, J.; Suh, Y. D.; Ham, J.; Ko, S. H. Highly Sensitive and Stretchable Multidimensional Strain Sensor with Prestrained Anisotropic Metal Nanowire Percolation Networks. *Nano Lett.* **2015**, *15*, 5240–5247.

(36) Jeong, C. K.; Lee, J.; Han, S.; Ryu, J.; Hwang, G. T.; Park, D. Y.; Park, J. H.; Lee, S. S.; Byun, M.; Ko, S. H.; et al. A Hyper-Stretchable Elastic-Composite Energy Harvester. *Adv. Mater.* **2015**, *27*, 2866–2875.

(37) Moon, H.; Lee, H.; Kwon, J.; Suh, Y. D.; Kim, D. K.; Ha, I.; Yeo, J.; Hong, S.; Ko, S. H. Ag/Au/Polypyrrole Core-Shell Nanowire Network for Transparent, Stretchable and Flexible Supercapacitor in Wearable Energy Devices. *Sci. Rep.* **2017**, *7*, 41981.

(38) Lee, J.; An, K.; Won, P.; Ka, Y.; Hwang, H.; Moon, H.; Kwon, Y.; Hong, S.; Kim, C.; Lee, C.; et al. A Dual-Scale Metal Nanowire Network Transparent Conductor for Highly Efficient and Flexible Organic Light Emitting Diodes. *Nanoscale* **2017**, *9*, 1978–1985.

(39) Park, J. H.; Han, S.; Kim, D.; You, B. K.; Joe, D. J.; Hong, S.; Seo, J.; Kwon, J.; Jeong, C. K.; Park, H. J.; et al. Plasmonic-Tuned Flash Cu Nanowelding with Ultrafast Photochemical-Reducing and Interlocking on Flexible Plastics. *Adv. Funct. Mater.* **2017**, *27*, 1701138.

(40) Jeong, S.; Cho, H.; Han, S.; Won, P.; Lee, H.; Hong, S.; Yeo, J.; Kwon, J.; Ko, S. H. High Efficiency, Transparent, Reusable, and Active PM2.5 Filters by Hierarchical Ag Nanowire Percolation Network. *Nano Lett.* **2017**, *17*, 4339–4346.

(41) Han, S.; Hong, S.; Yeo, J.; Kim, D.; Kang, B.; Yang, M. Y.; Ko, S. H. Nanorecycling: Monolithic Integration of Copper and Copper Oxide Nanowire Network Electrode through Selective Reversible Photothermochemical Reduction. *Adv. Mater.* **2015**, *27*, 6397–6403.

(42) Hong, S.; Lee, H.; Lee, J.; Kwon, J.; Han, S.; Suh, Y. D.; Cho, H.; Shin, J.; Yeo, J.; Ko, S. H. Highly Stretchable and Transparent Metal Nanowire Heater for Wearable Electronics Applications. *Adv. Mater.* **2015**, *27*, 4744–4751.

(43) Jung, J.; Lee, H.; Ha, I.; Cho, H.; Kim, K. K.; Kwon, J.; Won, P.; Hong, S.; Ko, S. H. Highly Stretchable and Transparent Electromagnetic Interference Shielding Film Based on Silver Nanowire Percolation Network for Wearable Electronics Applications. *ACS Appl. Mater. Interfaces* **2017**, *9*, 44609–44616.

(44) Gong, S.; Zhao, Y.; Yap, L. W.; Shi, Q.; Wang, Y.; Bay, J. A. P.; Lai, D. T.; Uddin, H.; Cheng, W. Fabrication of Highly Transparent and Flexible Nanomesh Electrode via Self-Assembly of Ultrathin Gold Nanowires. *Adv. Electron. Mater.* **2016**, *2*, 1600121.

(45) Ho, M. D.; Ling, Y.; Yap, L. W.; Wang, Y.; Dong, D.; Zhao, Y.; Cheng, W. Percolating Network of Ultrathin Gold Nanowires and Silver Nanowires toward “Invisible” Wearable Sensors for Detecting Emotional Expression and Apexcardiogram. *Adv. Funct. Mater.* **2017**, *27*, 1700845.

(46) Ho, M. D.; Liu, Y.; Dong, D.; Zhao, Y.; Cheng, W. Fractal Gold Nanoframework for Highly Stretchable Transparent Strain-Insensitive Conductors. *Nano Lett.* **2018**, *18*, 3593.

(47) Lu, N.; Wang, X.; Suo, Z.; Vlassak, J. Metal Films on Polymer Substrates Stretched Beyond 50%. *Appl. Phys. Lett.* **2007**, *91*, 221909.

(48) He, J.; Wang, Y.; Feng, Y.; Qi, X.; Zeng, Z.; Liu, Q.; Teo, W. S.; Gan, C. L.; Zhang, H.; Chen, H. Forest of Gold Nanowires: A New Type of Nanocrystal Growth. *ACS Nano* **2013**, *7*, 2733–2740.

(49) Amjadi, M.; Pichitpajongkit, A.; Lee, S.; Ryu, S.; Park, I. Highly Stretchable and Sensitive Strain Sensor Based on Silver Nanowire-Elastomer Nanocomposite. *ACS Nano* **2014**, *8*, 5154–5163.

(50) Kim, Y.; Zhu, J.; Yeom, B.; Di Prima, M.; Su, X.; Kim, J.-G.; Yoo, S. J.; Uher, C.; Kotov, N. A. Stretchable Nanoparticle Conductors with Self-Organized Conductive Pathways. *Nature* **2013**, *500*, 59–63.

(51) Chun, K. Y.; Oh, Y.; Rho, J.; Ahn, J. H.; Kim, Y. J.; Choi, H. R.; Baik, S. Highly Conductive, Printable and Stretchable Composite Films of Carbon Nanotubes and Silver. *Nat. Nanotechnol.* **2010**, *5*, 853–857.

(52) Moon, G. D.; Lim, G. H.; Song, J. H.; Shin, M.; Yu, T.; Lim, B.; Jeong, U. Highly Stretchable Patterned Gold Electrodes Made of Au Nanosheets. *Adv. Mater.* **2013**, *25*, 2707–2712.

(53) Matsuhisa, N.; Kaltenbrunner, M.; Yokota, T.; Jinnou, H.; Kuribara, K.; Sekitani, T.; Someya, T. Printable Elastic Conductors with a High Conductivity for Electronic Textile Applications. *Nat. Commun.* **2015**, *6*, 7461.

(54) Tybrandt, K.; Voros, J. Fast and Efficient Fabrication of Intrinsically Stretchable Multilayer Circuit Boards by Wax Pattern Assisted Filtration. *Small* **2016**, *12*, 180–184.

(55) Park, M.; Im, J.; Shin, M.; Min, Y.; Park, J.; Cho, H.; Park, S.; Shim, M. B.; Jeon, S.; Chung, D. Y.; Bae, J.; Park, J.; Jeong, U.; Kim, K. Highly Stretchable Electric Circuits from a Composite Material of Silver Nanoparticles and Elastomeric Fibres. *Nat. Nanotechnol.* **2012**, *7*, 803–809.

(56) Hu, L.; Yuan, W.; Brochu, P.; Gruner, G.; Pei, Q. Highly Stretchable, Conductive, and Transparent Nanotube Thin Films. *Appl. Phys. Lett.* **2009**, *94*, 161108.

(57) Mates, J. E.; Bayer, I. S.; Palumbo, J. M.; Carroll, P. J.; Megaridis, C. M. Extremely Stretchable and Conductive Water-Repellent Coatings for Low-Cost Ultra-Flexible Electronics. *Nat. Commun.* **2015**, *6*, 8874.

(58) Guo, R.; Yu, Y.; Xie, Z.; Liu, X.; Zhou, X.; Gao, Y.; Liu, Z.; Zhou, F.; Yang, Y.; Zheng, Z. Matrix-Assisted Catalytic Printing for the Fabrication of Multiscale, Flexible, Foldable, and Stretchable Metal Conductors. *Adv. Mater.* **2013**, *25*, 3343–3350.

(59) Guo, R.; Yu, Y.; Zeng, J.; Liu, X.; Zhou, X.; Niu, L.; Gao, T.; Li, K.; Yang, Y.; Zhou, F.; et al. Biomimicking Topographic Elastomeric Petals (E-Petals) for Omnidirectional Stretchable and Printable Electronics. *Adv. Sci.* **2015**, *2*, 1400021.

(60) Wang, X.; Hu, H.; Shen, Y.; Zhou, X.; Zheng, Z. Stretchable Conductors with Ultrahigh Tensile Strain and Stable Metallic Conductance Enabled by Prestrained Polyelectrolyte Nanoplayers. *Adv. Mater.* **2011**, *23*, 3090–3094.

(61) Yu, Y.; Yan, C.; Zheng, Z. Polymer-Assisted Metal Deposition (PAMD): A Full-Solution Strategy for Flexible, Stretchable, Compressible, and Wearable Metal Conductors. *Adv. Mater.* **2014**, *26*, 5508–5516.

(62) Ekman, P.; Friesen, W. V. *Unmasking the Face: A Guide to Recognizing Emotions from Facial Clues*; ISHK: Los Altos, CA, 2003.